Proceedings of the International Multiconference on
Computer Science and Information Technology pp. 759–766

ISBN 978-83-60810-27-9
ISSN 1896-7094

Real-Time Embedded Fault Detection Estimators in a Satellite's Reaction Wheels

Nicolae Tudoroiu
Concordia University
1455 De Maisonneuve Blvd. West,
Montreal, Quebec, Canada
Email: tnicolae@excite.com

Ehsan Sobhani-Tehrani
McGill University
805 rue Sherbrooke Ouest
Montreal, Quebec, Canada
Email:ehsan.sobhani@gmail.com

Kash Khorasani
Concordia University
1455 De Maisonneuve Blvd. West,
Montreal, Quebec, Canada
Email:kash@ece.concordia.ca

Tiberiu Letia
Technical University Cluj-Napoca
15 Constantin Daicoviciu Street,
Cluj-Napoca, Romania
Email:tsletia@gmail.com

Roxana-Elena Tudoroiu
Technical University Cluj-Napoca
15 Constantin Daicoviciu Street,
Cluj-Napoca, Romania
Email: tudelena@excite.com

***Abstract*— The main idea of this paper is the real-time implementation of the Fault Detection Kalman Filter Estimators (FDKFE) in a satellite's Reaction Wheels during its scientific mission. We assume that the satellite's reaction wheels are subjected to several failures due to the abnormal changes in power distribution, motor torque, windings current as well as the temperature caused by a motor current increase or friction. The proposed real-time FDKFE strategies consist of two embedded multiple model bank of nonlinear Kalman Filter (Extended/Unscented) estimators. This research work is based on our previous results in this field and we intend to extend this approach by real-time implementations of the developed FDKFE strategies (FDDM-EKF and FDDM-UKF). Furthermore we will construct a benchmark to compare their results to have an overall image how perform these strategies.**

I. Introduction

THE most important faults in the aerospace satellite's systems are the result of unexpected failures, interferences as well as the age of their crucial components. Also the defective measurement and control loops equipment, in particular some of the sensors and actuators should be considered. Whenever these critical situations come out the satellite's systems could lose the control, require much more energy, and could operate harmfully. Therefore to operate in real-time at high energy efficiency and to guarantee the equipment safety and reliability it is important to develop suitable FDKFE strategies able to detect and diagnose any time every faulty satellite's system components and consequently corrective and reconfiguration actions should be initiated promptly. Up to date for the majority part of the satellites, the onboard measurements data acquisition is sent to the land stations relatively frequently. However the operators still remain implicated to monitor some of the telemetry measurements and to diagnose the inconsistency of the operating equipment. Effectively the existing methods to identify and to adjust the equipment failures are mostly labor-intensive task, and consequently sustained, rhythmic and error-prone. In the majority situations the operators inspect telemetry plots manually to determine the satellite's reaction wheels health motors current. Also they use statistical evaluation that still necessitates considerable human knowledge, consequently error-prone that could generate harshly equipment operation. In these circumstances the problem of satellite monitoring and fault diagnosis becomes a critical issue, very complex that need to be implemented in mainframe environment using more sophisticated control systems and artificial intelligent strategies. Therefore the objective of our research is to develop more proficient, accurate and reliable real-time FDKFE strategies based on the nonlinear estimation techniques.

II. REACTION WHEEL's DYNAMICS

The Reaction Wheel (RW) model is developed based on detailed schematics shown in Figure 1 [3]. In a state-space representation associated to the RW actuator healthy mode (j=1) or its faulty modes ($j=\overline{1,N}$) we could write

(i) State Equation:

$$\begin{bmatrix} x_{j,1}(k+1) \\ x_{j,2}(k+1) \end{bmatrix} = \begin{bmatrix} T_s G_d \omega_d (f_1(x_{j,1}(k), x_{j2}(k)) - f_3(x_{j,2}(k)) \\ \dfrac{T_s[k_f x_{j,1}(k)(1+f_2(x_{j,2}(k))) - \tau_c f_4(x_{j,2}(k))]}{J} + (1 - \dfrac{T_s \tau_v}{J}) x_{j,2}(k) \end{bmatrix} + T_s \begin{bmatrix} G_d \omega_d u(k) \\ \dfrac{\tau_{noise}}{J} \end{bmatrix} + w_j(k) := F_j(x_{jk}, u_k) + w_{jk} \quad (1)$$

(ii) Output equation:

$$\begin{bmatrix} y_{j,1}(k) \\ y_{j,2}(k) \end{bmatrix} = \begin{bmatrix} 1 & 0 \\ 0 & 1 \end{bmatrix} \begin{bmatrix} x_{j,1}(k) \\ x_{j,2}(k) \end{bmatrix} + \upsilon_j(k) := H_j(x_{jk}, u_k) + v_{jk} \quad (2)$$

where the j-state vector mode is defined as:

$$x_j(k) := x_{jk} := \begin{bmatrix} x_{j,1}(k) \\ x_{j,2}(k) \end{bmatrix} = \begin{bmatrix} I_{m,j}(k) \\ \omega_{w,j}(k) \end{bmatrix} \quad (3)$$

The input command $u(k) = V_{com}$ is generated by the attitude controller, and it represents the command voltage applied to the reaction wheel motor axis. The functions H_s, H_b, H_f that appear in the reaction wheel diagram shown in Figure 1 represent the discontinuous Heaviside functions and the sign (.) block function represents the sign function. Also T_s is the sampling period of the discrete-time model of the reaction wheel actuator, w_{jk} and v_{jk} that appear in Figure 2 are the process and measurement noise, assuming that they are independent white Gaussian random processes with zero mean and covariance matrices:

$$E[w_n w_n^T] = \begin{cases} Q_w, n = k \\ 0, n \neq k \end{cases} \quad E[v_n v_n^T] = \begin{cases} R_v, n = k \\ 0, n \equiv k \end{cases} \quad (4)$$

The other parameters indicated in the model are identical to the reaction wheel parameters that are used in [3], and [6]-[9].

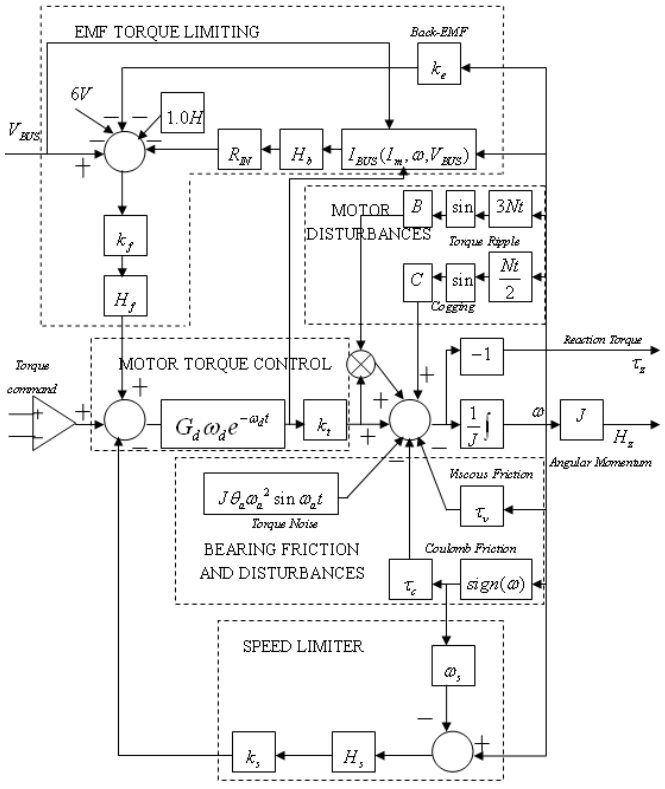

Fig.1 A detailed block diagram of a high fidelity reaction wheel model

III. Extended Kalman Filter Estimator (EKF)

Consider the dynamics of a linear stochastic system expressed in the state-space difference representation

$$x_{k+1} = Fx_k + Gu_k + w_k \quad (5)$$

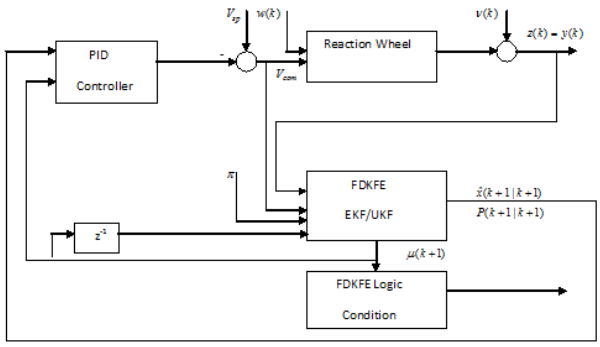

Fig. 2 The satellite's embedded FDKFE integrated structure

$$y_k = Hx_k + v_k \quad (6)$$

The process and measurement noise have normal probability distributions governed by

$$p(w) \sim N(0, Q_w)$$
$$p(v) \sim N(0, R_v) \quad (7)$$

The covariance matrices Q_w (process noise covariance) and R_v (measurement noise covariance) might change with each time step or measurement, but in our approach we assume that they are constant. Due to the process noise injected in the state space equation (5)-(6), the state vector $x_k \in R^n$ becomes random variable with its distribution approximated by a Gaussian distribution function $p(x) \sim G(\hat{x}, P_x)$.

Considering the nonlinear model of a reaction wheel as given by (1)-(2), the linearized state transition and observation matrices are defined according to the following Jacobeans

$$F_k = \frac{\partial f(x_k, u_k)}{\partial x_k}\Big|_{\hat{x}_{k-1|k-1}, u_k} = \begin{bmatrix} F_{11} & F_{12} \\ F_{21} & F_{22} \end{bmatrix}$$
$$H_k = \frac{\partial h(x_k, u_k)}{\partial x_k}\Big|_{\hat{x}_{k|k-1}, u_k} = \begin{bmatrix} 1 & 0 \\ 0 & 1 \end{bmatrix} \quad (8)$$

where G is an identity matrix. The EKF algorithm used for the state estimation of this dynamical system is now given according to the following steps [2]:

Step1. Initialization: for $k = 0$, set:

$\hat{x}_{0|0} = E[x_0]$, $P_{0|0} = E[(x_0 - \hat{x}_{0|0})(x_0 - \hat{x}_{0|0})^T]$ representing the distribution of initial state estimate and its covariance matrix

Step2. Prediction step: Predict the state and the estimated covariance according to

$$\hat{x}_{k|k-1} = f(\hat{x}_{k-1|k-1}, u_k)$$
$$P_{k|k-1} = F_k P_{k-1|k-1} F_k^T + Q_w \quad (9)$$

Step3. Update step:

3.1 Innovation or measurement residual

$$\tilde{y}_k = z_k - h(\hat{x}_{k|k-1}, u_k) \quad (10)$$

3.2 Innovation or residual covariance

$$S_k = H_k P_{k|k-1} H_k{}^T + R_v \tag{11}$$

3.3 Optimal Kalman filter gain

$$K_k = P_{k|k-1} H_k{}^T S_k{}^{-1} \tag{12}$$

3.4 Update state estimate

$$\hat{x}_{k|k} = \hat{x}_{k|k-1} + K_k \tilde{y}_k \tag{13}$$

3.5 Update estimate covariance

$$P_{k|k} = (I - K_k H_k) P_{k|k-1} \tag{14}$$

The covariance matrices Q_w (process noise covariance) and R_v (measurement noise covariance), together with the initial error covariance $P_{0|0}$ are the three tuning parameters in the EKF algorithm.

The matrices Q_w and R_v are determined empirically and account for uncertainty in the tracking data. Setting these matrices "properly" significantly contributes in making the EKF filter robust. The error covariance matrix P indicates uncertainty in the state estimate and provides criterion for the error bound.

IV. The unscented kalman filter estimator (UKF)

The Unscented Kalman Filter (UKF) is based on the unscented transformation (UT) which addresses the general problem of state estimation of a system that is governed by a nonlinear stochastic difference state-space representation [2], [4]-[5]:

$$\begin{aligned} \mathbf{x}_{k+1} &= F(\mathbf{x}_k, \mathbf{u}_k) + \mathbf{w}_k \\ \mathbf{y}_k &= H(\mathbf{x}_k, \mathbf{u}_k) + \mathbf{v}_k \end{aligned} \tag{15}$$

The critical operation that is performed in the Kalman filter is propagation of a Gaussian random state variable $\mathbf{x}_k \in \mathbf{R}^n$ through the system dynamics. In the Extended Kalman Filter (EKF) estimator the Gaussian random state variable is propagated analytically through the first-order linearization of the nonlinear system. This can introduce large errors in the true *a posterior* mean and covariance of the transformed Gaussian random state variable, leading to sub-optimal performance and sometimes divergence of the EKF estimator.

The UKF estimator is developed as an alternative to the EKF estimator and addresses this problem by using a deterministic sampling approach.

Using the principle that a minimal set of carefully chosen weighted sample points, called sigma points, can be used to parameterize mean and covariance, the UKF estimator yields superior performance when compared to the EKF estimator, especially for nonlinear systems.

These sigma points should completely capture the true mean and covariance of the Gaussian random state variable, and are propagated through the true nonlinear system dynamics. In it was shown that a random *n*-dimensional state variable x with mean $\bar{x}$ and covariance P could be approximated by $2n+1$ weighted sigma points X_i, $i = 1,....,2n+1$, that are given by:

$$\begin{aligned} X_0 &= \bar{x} \ , \ W_0 = \frac{k}{n+k} \\ X_i &= \bar{x} + (\sqrt{(n+k)P})_i \ , \ W_i = \frac{1}{2(n+k)} \\ X_{i+n} &= \bar{x} - (\sqrt{(n+k)P})_i \ , \ W_{i+n} = \frac{1}{2(n+k)} \end{aligned} \tag{16}$$

where k is a scalar that provides an extra degree of freedom for "fine tuning" the higher order moments of the approximation, and can be used to reduce the overall prediction error, $(\sqrt{(n+k)P})_i$ is the *i*-th row or column of the matrix square root of $(n+k)P$, and W_i is the weight associated with the $i-th$ point X_i.

The cloud of the transformed sigma points distribution X_{k+1} given by

$$X_{k+1} = F(X_k, u_k) \tag{17}$$

captures the *a posterior* mean that is given by the weighted average of the transformed sigma points:

$$\bar{x} = \sum_{i=0}^{2n} W_i X_{k+1,i} \tag{18}$$

and the covariance (the weighted outer product of the transformed sigma points) given by

$$P = \sum_{i=0}^{2n} W_i (X_{k+1,i} - \bar{x})(X_{k+1,i} - \bar{x})^T \tag{19}$$

In some applications the sampling rate could be an important source of degrading the UKF estimator performance.

The main advantage of the UKF estimator is that it is suitable for most general class of process models, due to the fact that the mean and covariance are calculated using standard vector matrix operations, and the implementation is extremely fast since UKF does not require calculation of Jacobean matrices that could in certain cases lead to numerical complications and difficulties.

Also the sigma points capture the mean and the covariance irrespective of the choice of matrix square root that is used.

Numerically efficient and stable methods such as the Cholesky decomposition [5] can be used for this purpose.

Similar to EKF estimator the UKF estimator design steps for the both phases (prediction and correction) are well presented in figure 3.

V. Fault Detection Strategy Design

The multiple model approach for fault detection and diagnosis assumes that the actual system at any time can be modeled sufficiently accurately by the following jump Markov hybrid nonlinear system [1]:

$$\begin{aligned} x(k+1) &= F(k, m(k+1), x(k), u(k)) + T(k, m(k+1)) w(k, m(k+1)) \\ x(0) &: \ N(\hat{x}_0, P_0) \\ z(k) &= G(k, m(k), x(k), u(k)) + v(k, m(k)) \end{aligned} \tag{20}$$

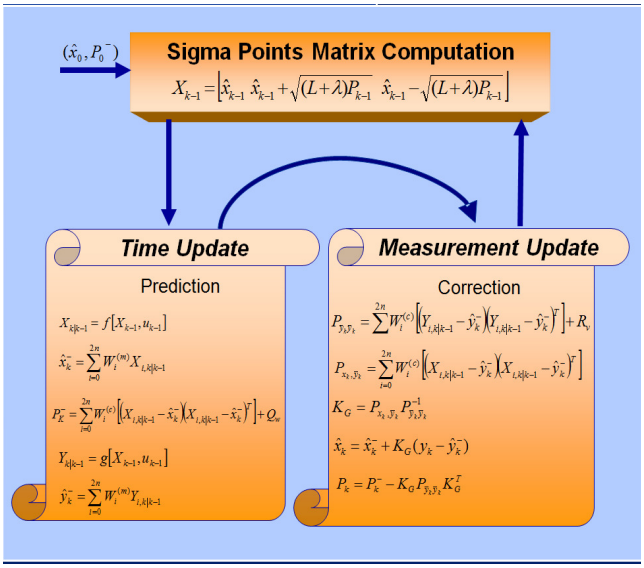

Fig. 3 The block scheme of the UKF estimator

The mode of the system (normal or faulty) at time k is selected by a discrete process m_j and modeled as a s-state, first-order Markov chain with transition probabilities $\pi_{ij}(k)$ given by:

$$\pi_{ij}(k) = P\{m_j(k+1) \mid m_i(k)\},\ \forall m_i, m_j \quad S \qquad (21)$$

and

$$0 \le \pi_{ij}(k) \le 1,\ i = \overline{1,N},\ j = \overline{1,N},\qquad \sum_j \pi_{ij}(k) = 1,\ \ i = \overline{1,N} \qquad (22)$$

The initial state distribution of the Markov chain is $\pi(0) = [\pi_1\ \pi_2\ \pi_3 \ldots\ldots \pi_N]$, where

$$0 \le \pi_j \le 1,\ \forall j = \overline{1,N},\ \sum_{j=1}^{N} \pi_j = 1 \qquad (23)$$

and where $x(k)$ is the state vector, $z(k)$ is the mode-dependent measurement vector, and $u(k)$ is the control input vector. The process and measurement noise vectors $w(k)$ and $v(k)$, respectively, are mutually independent, additive, white Gaussian of zero mean and covariance matrices $Q_w(k)$ and $R_v(k)$, and are independent of the initial state $x(0)$. In expression (44), P{.} denotes the probability operator. The event that m_j is in effect at time k is denoted as $m_j(k) = \{m(k) = m_j\}$, and $S = \{m_1, m_2, ..., m_N\}$ represents the set of all possible system modes. The system may jump from one such system to another at a random time. It can be observed from that the state vector observations are in general noisy and dependent. Therefore, the mode information is embedded in the measurement sequence. The system mode sequence is an indirectly observed Markov chain, from which the transition probability matrix $\pi = \{\pi_{ij}\}$ represents a design parameter. The simulation results and our comparative studies are presented in the next section.

The root-causes of faults injected in the reaction wheels are due to the following sources:

(i) unexpected viscous friction changes generating anomalies in the temperature T,

(ii) unexpected changes in the bus voltage V_{bus},

(iii) loss of effectiveness in the motor torque as represented by unexpected changes in the coefficient k_t.

The FDKFE strategy for the hybrid system can be stated as that of determining the current model state. In other words, it involves determining whether the normal or a faulty mode is currently in effect from a sequence of noisy observations. How to design set of modes to represent the possible system modes is a key issue in multiple model approach, which is problem-dependent. This design should be achieved by attempting to have models (approximately) that represent or cover all possible system modes at any given time. This represents the model set design that is critical for multiple model based FDKFE. To design a good set of models requires *a priori* knowledge of possible faults in the system. In application of multiple model estimation techniques for fault detection and diagnosis, the following tasks should be implemented [1]:

a) model set design,
b) filter selection,
c) estimate fusion, and
d) filter re-initialization.

Filter selection deals with the problem of selecting a model-based recursive filter such as Kalman Filter for each model of the nonlinear system. The estimate fusion task combines model-conditional estimates to obtain an overall estimate. Towards this end, three approaches could be investigated, namely soft, hard and random decisions. The procedure for reinitializing each single-model based filter from time to time is of significant importance for multi-model estimation. The simplest approach for reinitializing each filter is to use its previous state estimate and filter covariance at the current cycle. In this case filters are operating in parallel and no interactions exist among them.

However, this may lead to unsatisfactory performance when the system structure or its mode changes. For this reason, it would be more appropriate to reinitialize each filter using the previous overall state estimate and covariance matrix which does lead to an interacting multiple model estimation technique. For each faulty mode corresponding to a set of possible ACS reaction wheel faults and a normal operating mode, one can apply an unscented Kalman filter based on measurements collected from reaction wheels angular velocity vector$\boldsymbol{\varpi}$. The input considered can be taken as the torque command voltage vector *u* that is generated by, e.g. a PID controller. The dynamics of an unscented Kalman filter associated with each mode is described by the following nonlinear state space representation:

$$\begin{aligned} x_j(k+1) &= F_j(k, x_j(k), u_j(k)) + T_j(k) w_j(k) \\ z_j(k) &= G_j(k, x_j(k), u_j(k)) + v_j(k) \end{aligned} \qquad (24)$$

where $x_j = \boldsymbol{\varpi}(k)$ and the subscript j denotes the quantities pertaining to mode m_j. The nonlinear functions F_j, G_j and

the weighting matrix T_j may have different structures for different values of j. The process noise and measurement noise vectors w_j and v_j are white Gaussian of zero mean with covariance matrices Q_{wj} and R_{vj}, respectively. In principle the probability of a given model matches the system mode provides the required information for the fault detection and diagnosis. Taking into account historical behavior of modes at time ***k*** ensures that the interacting multiple model algorithm yields a good estimate.

Consequently, exponential increase in complexity of a detection algorithm is avoided by mixing previous estimates at beginning of each cycle.

The model probabilities provide an indication of the mode in effect at any given time, and therefore can provide an indication of the reaction wheel actuator fault. By using model probabilities information, both fault detection and diagnosis can be achieved. This decision making process is formally stated according to:

$$\begin{aligned} &\mu_j(k+1)=\max_j \mu_j(k+1)=\mu \\ &If \quad \mu>\mu_T \quad then \quad \text{mode } j \quad is \quad faulty \\ &Otherwise \quad no \quad fault \quad occurs \end{aligned} \tag{25}$$

where $\mu_{Threshold}$ represents the fault detection threshold value. The interacting estimation algorithm runs each parallel filter banks only once in each cycle. Each of these filters at time $t_{k+1} = k+1$ has its own input, the state estimate at time t_k, $\hat{x}^0(k|k)$, and its own covariance matrix, $P^0(k|k)$, which form a valid quasi-sufficient statistics of all the past information, under the assumption that model of each filter matches the system mode.

The above decision rule yields not only fault detection capability but also information about the type (sensor or actuator), the location (which sensor or actuator), the size (total failure or partial failure with fault severity), and the fault occurrence time.

VI. Nhe Embedded Fault Detection Kalman Filter Estimators Interacting Strategy

The embedded structure of an Interactive Multiple Model algorithm and EKF/UKF estimators is included in the references [1]-[2], [4]-[9]. Due to space limitations only the UKF based procedures is described below, the algorithm steps remaining almost the same for the both cases.

Step 1: Interaction and mixing of the estimates [1]

1.1 Compute the predicted mode probability from k to $k+1$

$$\hat{\mu}_j(k+1|k)=\sum_1^N \pi(i,j)\mu_i(k) \tag{26}$$

1.2 Compute the mixing probability at k:

$$\mu_{ij}(k)=\frac{\pi(i,j)\quad \mu_i(k)}{\hat{\mu}_j(k+1|k)} \tag{27}$$

1.3 Compute the mixing estimate at k:

$$\hat{x}_{j0}(k|k)=\sum_1^N \hat{x}_i(k|k)\times\mu_{ij}(k) \tag{28}$$

1.4 Compute the mixing covariance at k, that is, P_0

$$P_{j0}(k|k)=\sum_1^N [P_i(k|k)+(\hat{x}_{j0}(k|k)-\hat{x}_i(k))(\hat{x}_{j0}(k|k)-\hat{x}_i(k|k))^T]\times\mu_{ij}(k) \tag{29}$$

Step 2: Model conditional filtering [1]

(i) Prediction step [2], [4]-[5]:

2.1 Compute the global state sigma points matrix:

$$X_{k|k}=[\hat{x}(k|k)\quad \hat{x}(k|k)+\sqrt{(L+\lambda)P(k|k)}\quad \hat{x}(k|k)-\sqrt{(L+\lambda)P(k|k)}] \tag{30}$$

where the state covariance matrix $P(k|k)$ is updated for each time increment.

2.2 Compute the transformed global state sigma points matrix from k to $k+1$:

$$X_{k+1|k}=F(k,X_{k|k},u_k) \tag{31}$$

2.3 Compute the predicted global state from k to $k+1$:

$$\hat{x}(k+1|k)=\sum_{i=0}^{2n} W_i^{(m)} X_{i,k+1|k} \tag{32}$$

2.4 Compute the global predicted covariance from k to $k+1$:

$$\begin{aligned} P(k+1|k)=&(W_0^{(c)}+1-\alpha^2)(X_{0,k+1|k}-\hat{x}(k+1|k))(X_{0,k+1|k}-\hat{x}(k+1|k))^T+\\ &+\sum_{i=1}^{2n} W_i^{(c)}[(X_{i,k+1|k}-\hat{x}(k+1|k))(X_{i,k+1|k}-\hat{x}(k+1|k))^T]+Q_w \end{aligned} \tag{33}$$

2.5 Compute the transformed global output sigma points matrix from k to $k+1$:

$$Y_{k+1|k}=G(k,X_{k+1|k},u_k) \tag{34}$$

2.6 Compute the predicted global output from k to $k+1$

$$\hat{y}(k+1|k)=\sum_{i=0}^{2n} W_i^{(m)} Y_{i,k|k-1} \tag{35}$$

2.7 Compute the measurement residual for each mode j at $k+1$:

$$v_j(k+1)=z(k+1)-\hat{y}_j(k+1|k) \tag{36}$$

where $\hat{x}_j(k+1|k)$ represents the j-th component of the global predicted state $\hat{x}(k+1|k)$ (the mode j), and $z(k+1)$ represents the new available measurement for the active mode in effect, let say i, namely

$$z(k+1)=z_i(k+1) \tag{37}$$

2.8 Compute the global predicted output covariance matrix $P_{\tilde{y}\tilde{y}}(k+1|k)$

$$\begin{aligned} P_{\tilde{y}\tilde{y}}(k+1|k)=&(W_0^{(c)}+1-\alpha^2)(Y_{0,k|k-1}-\hat{y}(k+1|k))(Y_{0,k|k-1}-\hat{y}(k+1|k))^T+\\ &+\sum_{i=1}^{2n} W_i^{(c)}[(Y_{i,k|k-1}-\hat{y}(k+1|k))(Y_{i,k|k-1}-\hat{y}(k+1|k))^T]+R \end{aligned} \tag{38}$$

2.9 Compute the global cross-covariance matrix

$$\begin{aligned} P_{\tilde{x}\tilde{y}}(k+1|k)=&(W_0^{(c)}+1-\alpha^2)(X_{0,k|k-1}-\hat{x}(k+1|k))(Y_{0,k|k-1}-\hat{y}(k+1|k))^T+\\ &+\sum_{i=1}^{2n} W_i^{(c)}[(X_{i,k|k-1}-\hat{x}(k+1|k))(Y_{i,k|k-1}-\hat{y}(k+1|k))^T] \end{aligned} \tag{39}$$

2.10 Compute the global Kalman filter gain at k+1**:**

$$K_G(k+1) = P_{\tilde{x}\tilde{y}}(k+1 \mid k)(P_{\tilde{y}\tilde{y}}(k+1 \mid k))^{-1} \quad (40)$$

(ii) Correction step:

2.11 Update the state estimated at k+1

$$\hat{x}_j(k+1 \mid k+1) = \hat{x}_j(k+1 \mid k) + K_{G,j}(k+1)\nu_j(k+1) \quad (41)$$

2.12 Update the state covariance matrix

$$P_j(k+1|k+1) = P_j(k+1|k) - K_{G,j}(k+1)(P_{\tilde{y}\tilde{y}}(k+1|k))^{-1}(K_{G,j}(k+1))^T \quad (42)$$

Step 3: Update the mode probability at k+1

3.1 Compute the likelihood function at k+1

$$L_j(k+1) = \frac{1}{\sqrt{|(2\pi)P_{j,\tilde{y}\tilde{y}}(k+1|k)|}} \exp[-\frac{1}{2}\nu_j^T(k+1)(P_{j,\tilde{y}\tilde{y}}(k+1|k))^{-1}\nu_j(k+1)] \quad (43)$$

3.2 Update the mode probability at k+1:

$$\mu_j(k+1) = \frac{\mu_j(k+1 \mid k) L_j(k+1)}{\sum_1^N \mu_j(k+1 \mid k) L_j(k+1)} \quad (44)$$

Step 4: Fault detection at k+1

4.1 Compute the mode probability vector at k+1:

$$\vec{\mu}(k+1) = \left[\mu_1(k+1) \;\; \mu_2(k+1) \;\; \mu_3(k+1) \ldots \mu_N(k+1)\right] \quad (45)$$

4.2 Obtain the maximum value of the mode probability vector:

$$\mu_{FDD\ \max} = \max_j \{\mu_j(k+1))\,, \quad (46)$$

4.3 Determine the index of the maximum value of mode probability vector

$$j = find(\vec{\mu} == \max(\vec{\mu})) \quad (47)$$

and subsequently assign:

$$index = j \quad (48)$$

Step 5: Fault decision – FDD logic

$$if \quad \mu_{FDD\max} > \mu_{Threshold} \quad \text{the fault occurs,} \quad (49)$$

Otherwise no fault occurs.

VII. Real-Time Control and FGKE Strategy Implementation

The control system literature rarely includes extensively the real-time software and hardware implementation aspects, and it doesn't pay attention beyond algorithms and sampling time selection. Normally the implementation aspect and real-time system design are connected together but in the most cases this connection is always ignored. Moreover the real-time system design is treated from control perspective ignoring the implementation aspects of the control algorithms. However in the last years the real-time implementation and design aspects get more transparency to control engineering field due to advent of software tools like MATLAB/SIMULINK with its RTW (Real-Time Workshop) and the RTWT (Real-Time Windows Target) Toolboxes. Definitely these new real-time platforms do the implementation of real-time experiments easier and save much time but on the other hand they have some drawbacks regarding a good insight view of the real-life problems that could emerge during the real-time implementation of the control system. Building a real-time ACS requires normally two stages: PID controller and estimators design as well as their digital implementations. At controller and estimators design stage some performance indices are defined and the PID controller and EKF and UKF estimators are designed to optimize these indices.

At implementation stage, multiple control tasks should be scheduled to run the FPGA (*Field-Programmable Gate Array*) onboard microprocessor or controller module. We have to take care about task scheduling taking into account the limited available computing resources. Firstly to select the sampling time T_s, it should take into account the limited computation time provided by the hardware such that to avoid the conflict with its computation time delay (control latency). Since the control latency is typically affected by control jitter, delay and loss can occur alternatively in the system at different instants of time. The loss of the ACS control signal $u(k)$ leads to the controller computer failure, unable to update its output during any one sampling interval, and accordingly the one step delayed input $u(k-1)$ it will be applied again. Since this situation may well occur accidentally at any instant of time, the failure to deliver a control signal can be treated as a casual ACS input disturbance $u_p(k)$. Anyway this interaction between control performance and task scheduling will be investigated in the future work.

VIII. Simulation Results

The real-time platform used to perform these real-time simulations was a MATLAB R2007b with SIMULINK running on the two processors WINDOWS OS machine. The simulation results are obtained for a sampling time T_s equal to 1s, but a carefully selection of it and the interaction between control performance and task scheduling will be done in the future work. In spite of a large number of scenarios, to have an overall image about the estimator's performance, we present in figures (4)-(5) only the partial simulation results for the both real-time embedded fault detection strategies. In these figures we will present in terms of the mode probability index the transient and the steady state of different fault modes occurrences in a multi-fault sequence. These figures reveal in the same time the robustness of the both estimators to the noise level and to the probability matrix. Also the estimator's performance comparison is available in the benchmark presented in Table 1.

IX. Conclusions

In this paper, we have studied the possibility of using two interactive multiple models based on Extended and Unscented Kalman Filter estimators to detect and diagnose the faults in reaction wheels of the attitude control system (ACS) in a satellite. The main contributions in our research are summarized briefly as follows:

(a) Detection and identification of reaction wheel faults of the ACS due to a number of possible

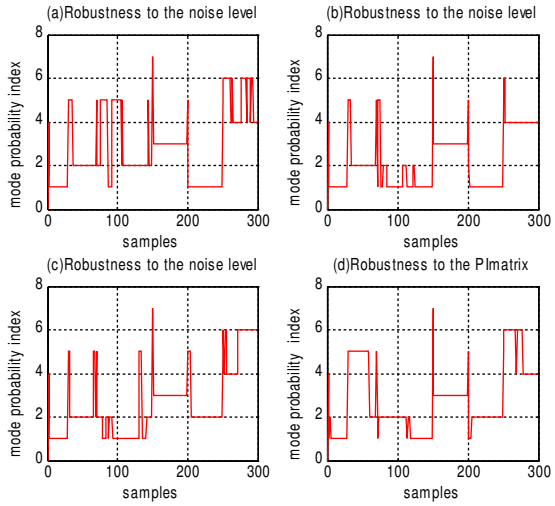

Fig. 4 The performance in terms of mode probabilities index for robustness analysis using the FD-EKF strategy

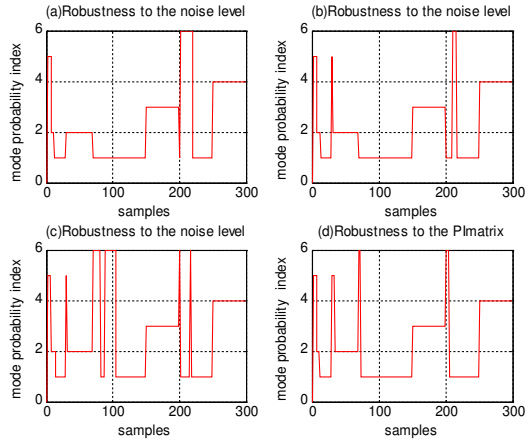

Fig. 5 The performance in terms of mode probabilities index for robustness analysis using the FD-UKF strategy

TABLE 1
THE PERFORMANCE COMPARISON OF THE FDKFE STRATEGIES

Item	Performance	KF	EKF	UKF
1	Accuracy Degree for modeled faults	Very good	Good	Very Good
2	Accuracy Degree for un-modeled faults	Small	Small	Good
3	Robustness to R ,Q matrices	Not Robust	Not Robust	Robust
4	Robustness to the matrix probabilities, π	Not Robust	Not Robust	Robust

*Embedded estimators: KF-Standard Kalman Filter, EKF-Extended Kalman Filter, UKF-Unscented Kalman Filter.

sources that generate soft and hard anomalies during a scientific mission of a satellite,

(b) Implementation of a bank of real-time parallel Kalman filters for faulty modes covering a quite large set of the most likely and commonly possible scenarios of reaction wheel failures,

(c) Detection and diagnosis of both partial and significant reaction wheel failures for different scenarios using the real-time EKF and UKF estimation algorithms,

(d) Comparison of performance capabilities and advantages of real-time UKF estimation algorithm with respect to the real-time EKF estimation algorithm, and

(e) Robustness analysis of both real-time estimation algorithms to the selection of model transition probabilities, modeling errors, and noise statistics under different scenarios.

The approach proposed in this paper is probabilistic in nature and yields results that are more accurate and having good fault classification capabilities than the spectral analysis that is well studied in the literature. Based on fault identification analysis that is carried it can be observed that the real-time UKF estimation algorithm is robust to modeling uncertainties, and to statistics of noise measurements and process noise. The both real-time algorithms work similar to a real-time neural network estimator and classifier employed to perform satisfactory FDKFE. Compared to a real-time neural network estimator and classifier, the real-time UKF estimation algorithm doesn't need an on-line training that takes an extensive amount of computational resources. Compared to the above approaches and real-time EKF estimation algorithm, the real-time UKF estimation algorithm performs better and has a much less computational burden and complexity, and it furthermore operates much faster. Perhaps the biggest drawback of predictive model-based approaches is the need for a suitable quantity of data for training and testing the system during the development phase [10], [13]. Moreover, stability of the real-time UKF estimation algorithm still remains an open question, which needs further investigation. Also, the behavior of the real-time UKF estimation algorithm for diagnosis in a fast or rapidly changing process dynamics needs to be explored further.

REFERENCES

[1]. Y. Zhang and Rong-Li Xiao, "Detection and Diagnosis of Sensor and Actuator Failures using IMM Estimator", *IEEE Transaction on Aerospace and Electronic Systems*, Vol.34, No.4, pp. 1293-1311, 1998.

[2]. S. Haykin, *Kalman Filtering and Neural Networks*, John Willey & Sons, 2001.

[3]. B. Bialke, "High Fidelity Mathematical Modeling of Reaction Wheel Performance", *Advances in the Astronautical Sciences*, 1998, pp. 483-496.

[4]. S. J. Julier and J. K. Uhlman, "A New Extension of the Kalman Filter to Nonlinear Systems". *Proceedings of AeroSense, Proceedings of the11th International Symposium on Aerospace/Defense Sensing, Simulation and Controls*, 1997, pp.182-193.

[5]. E. A. Wan, R. Merwe, "The Unscented Kalman Filter for Nonlinear Estimation", *Proceedings IEEE Symposium,* Alberta, Canada, 2000.

[6]. N. Tudoroiu and K. Khorasani, "Fault Detection and Diagnosis for Reaction Wheels of Satellite's Attitude Control System Using a Bank of Kalman Filters", *Proceedings of IEEE International Symposium on Signal, Circuits and Systems*, Iasi, Romania, 2005, pp. 199-202.

[7]. N. Tudoroiu and K. Khorasani, "Fault Detection and Diagnosis for Satellite's Attitude Control System using an Interactive Multiple Model (IMM) Approach", *Proceedings of the Conference on Control Applications*, Toronto, Canada, 2005.

[8]. N.Tudoroiu, K. Khorasani, "Satellite Fault Diagnosis using a Bank of Interacting Kalman Filters", *IEEE Transactions on Aerospace and Electronic Systems*, Vol. 43, No.4, 2007, pp. 1334-1350.

[9]. N. Tudoroiu, E. Sobhani-Tehrani, and K. Khorasani, "Interactive Bank of Unscented Kalman Filters for Fault Detection and Isolation in Reaction Wheel Actuators of Satellite Attitude Control System", *IECON'2006,The 32nd Annual Conference of the IEEE Industrial Electronics Society*, 2006.

[10]. J. D. Boskovic and K. M. Mehra, 2001, "Hybrid Fault Tolerant Control of Aerospace Vehicle", *Proceedings of the IEEE International Conference on Control Applications*, Mexico, 2001, pp.441-446.

[11]. Z. Li, L. Ma, and K. Khorasani, "Fault Detection in Reaction Wheel of a Satellite using Observer-based Dynamic Neural Networks", *Proceedings of International Symposium on Neural Networks*, 2005.

[12]. E. Sobhani, K. Khorasani, and S. Tafazoli, "*Dynamic Neural Network-based Estimator for Fault Diagnosis in Reaction Wheel Actuator of Satellite Attitude Control System*", *Proceedings of the International Joint Conference on Neural Networks*, 2005.

[13]. R. J. Patton, P. M. Frank, and R. N. Clark, "Fault Diagnosis in Dynamic Systems, Theory and Applications", Englewood Cliffs, NJ: Prentice Hall, 1989.